Dynamic pseudopotential theory of phonons in twelve cubic metals

Y. R. Wang and A. W. Overhauser
Department of Physics, Purdue University, West Lafayette, Indiana 47907
(Received 14 July 1986)

The dynamic pseudopotential model for phonons in metals involves division of each ion into an inner-ion core and a last-filled electron shell. Vibrations of the cores and shells have different amplitudes. Only Coulomb interactions, screened by the conduction-electron sea, enter the theory. The core and shell pseudopotentials involve just one parameter each, and these are determined phenomenologically for Na, K, Rb, Cu, Ag, Au, Ca, Sr, Ba, Yb, Al, and Pb. Distortion of the ions is found to be very important in the heavy metals. A recently discovered anomaly in the phonon dispersion of Ba can be attributed to exchange interactions between the (last-filled) shell and the conduction-electron sea. The (so far unmeasured) spectra for fcc Sr and bcc Yb are predicted.

I. INTRODUCTION

The dynamic pseudopotential model for phonons in metals, developed in a previous paper[1] (hereafter referred to as WO), is applied to twelve monatomic, cubic metals. The fundamental idea is to divide each ion into a core and a last-filled electron shell so that distortion of the ion during vibration can be included in the theory.[2] All interactions, core-core, core-shell, and shell-shell, are Coulombic. However, they are screened by the dielectric response of the conduction-electron sea. Exchange interactions between shell electrons and conduction electrons lead to three distinct dielectric functions: $\epsilon_{cc}(q)$, $\epsilon_{cs}(q)$, and $\epsilon_{ss}(q)$. The first one is the ordinary electron-gas dielectric function. The two remaining were derived in WO.

During a lattice vibration the core and shell displacements, $\mathbf{u}(\mathbf{L})$ and $\mathbf{v}(\mathbf{L})$, differ:

$$\mathbf{u}(\mathbf{L})=A\hat{\boldsymbol{\alpha}}_{\mathbf{q}}\cos(\mathbf{q}\cdot\mathbf{L}-\omega t)\ ,$$
$$\mathbf{v}(\mathbf{L})=B\hat{\boldsymbol{\beta}}_{\mathbf{q}}\cos(\mathbf{q}\cdot\mathbf{L}-\omega t)\ . \tag{1}$$

$\hat{\boldsymbol{\alpha}}_{\mathbf{q}}$ and $\hat{\boldsymbol{\beta}}_{\mathbf{q}}$ are unit polarization vectors. The dynamical matrix for a monoatomic Bravais lattice will be 6×6. The equations of motion were shown (in WO) to be

$$\begin{bmatrix} D(cc) & D(cs) \\ D(sc) & D(ss) \end{bmatrix}\begin{bmatrix} A\hat{\boldsymbol{\alpha}} \\ B\hat{\boldsymbol{\beta}} \end{bmatrix}=\begin{bmatrix} nM\omega^2A\hat{\boldsymbol{\alpha}} \\ znm\omega^2B\hat{\boldsymbol{\beta}} \end{bmatrix}, \tag{2}$$

where n is the density of atoms (of mass M) and z is the number of electrons in each (last-filled) shell. The 3×3 D's are

$$D_{ij}(cc)=4\pi n^2\left[\sum_{\mathbf{G}}\frac{|\rho_c(\mathbf{G}+\mathbf{q})|^2(\mathbf{G}+\mathbf{q})_i(\mathbf{G}+\mathbf{q})_j}{|\mathbf{G}+\mathbf{q}|^2\epsilon_{cc}(\mathbf{G}+\mathbf{q},\omega)}-{\sum_{\mathbf{G}}}'\left[\frac{|\rho_c(\mathbf{G})|^2}{\epsilon_{cc}(\mathbf{G},\omega)}+\frac{\rho_c(\mathbf{G})\rho_s(\mathbf{G})}{\epsilon_{cs}(\mathbf{G},\omega)}\right]\frac{\mathbf{G}_i\mathbf{G}_j}{G^2}\right]. \tag{3}$$

$\rho_c(Q)$ and $\rho_s(Q)$ are Fourier transforms of the core and shell pseudocharge densities, and will be discussed in Sec. II. The prime on the last sum (over reciprocal lattice vectors $\mathbf{G}$) indicates deletion of the term for $\mathbf{G}=0$:

$$D_{ij}(cs)=4\pi n^2\sum_{\mathbf{G}}\frac{\rho_c(\mathbf{G}+\mathbf{q})\rho_s(\mathbf{G}+\mathbf{q})(\mathbf{G}+\mathbf{q})_i(\mathbf{G}+\mathbf{q})_j}{|\mathbf{G}+\mathbf{q}|^2\epsilon_{cs}(\mathbf{G}+\mathbf{q},\omega)}\ . \tag{4}$$

$D(sc)$ is the transpose of $D(cs)$; and $D(ss)$ can be obtained from Eq. (3) by interchanging c and s.

The three lowest eigenfrequencies of Eq. (2) are phonon modes. For these solutions the $\omega=0$ limits of $\epsilon(q,\omega)$ can be used (because $\omega\ll\omega_p$, the conduction-electron plasma frequency). The three high-frequency modes of Eq. (2) are collective shell excitons. They describe vacuum-ultraviolet (15–90 eV) oscillations of the shells relative to the cores. For these solutions $\epsilon\approx1-\omega_p^2/\omega^2$. We will discuss the three ϵ's in greater detail below, but first we will choose models for the charge densities $\rho_c(\mathbf{r})$ and $\rho_s(\mathbf{r})$.

II. PSEUDOCHARGE DENSITIES: $\rho_c(\mathbf{r})$ AND $\rho_s(\mathbf{r})$

Our objective is to find models for the pseudocharge densities of the cores and shells which contain as much physics as possible but have a minimum number of parameters. We shall avoid (deliberately) any possibilities that involve discontinuities in charge density (or potentials resulting therefrom). Such pathology is not only unrealistic, but can lead to poor convergence of the $\mathbf{G}$ sums in Eqs. (3) and (4).

The nuclear charge is screened by $Z-z-v$ electrons, where Z is the atomic number, z the number of electrons in the shell, and v the valence, i.e., the number of conduction electrons per atom. A one-parameter charge distribution for the core will be chosen:

$$\rho_c(r)=e(z+v)(2\pi)^{-3/2}R_c^{-3}\exp(-r^2/2R_c^2)\ . \tag{5}$$

Its Fourier transform is

$$\rho_c(Q)=e(z+v)\exp(-R_c^2Q^2/2) . \quad (6)$$

The only (undetermined) parameter involved is R_c.

Shell charge densities can easily reflect the behavior appropriate to a given orbital angular momentum near $r=0$. Accordingly, for two electrons in an $l=0$ shell,

$$\rho_s(r)=-2e(2\pi)^{-3/2}R_s^{-3}\exp(-r^2/2R_s^2) , \quad (7)$$

where R_s is the shell "radius" parameter. The Fourier transform of Eq. (7) is,

$$\rho_s(Q)=-2e\exp(-R_s^2Q^2/2) . \quad (8)$$

The six electrons of a p shell will have an extra r^2 factor:

$$\rho_s(r)=-6e[(2\pi)^{-3/2}/3]R_s^{-5}r^2\exp(-r^2/2R_s^2) . \quad (9)$$

The Fourier transform is

$$\rho_s(Q)=-6e(1-R_s^2Q^2/3)\exp(-R_s^2Q^2/2) . \quad (10)$$

The ten electrons of a d shell will have an r^4 factor:

$$\rho_s(r)=-10e[(2\pi)^{-3/2}/15]R_s^{-7}r^4\exp(-r^2/2R_s^2) . \quad (11)$$

The Fourier transform is,

$$\rho_s(Q)=-10e[1-(2Q^2R_s^2/3)+Q^4R_s^4/15]\exp(-R_s^2Q^2/2) . \quad (12)$$

Finally, the fourteen electrons of an f shell have an r^6 factor:

$$\rho_s(r)=-14e[(2\pi)^{-3/2}/105]R_s^{-9}r^6\exp(-r^2/2R_s^2) , \quad (13)$$

which has a Fourier transform,

$$\rho_s(Q)=-14e[1-Q^2R_s^2+(Q^4R_s^4/5)-Q^6R_s^6/105]\exp(-R_s^2Q^2/2) . \quad (14)$$

As was the case for $\rho_c(r)$, the pseudo-ion-shell charge density has only one (undetermined) parameter: R_s.

The two parameters, R_c and R_s, of our pseudo-ion model will be determined by fitting the theory of WO, reviewed in Sec. I, to measured frequencies at the symmetry points on the Brillouin-zone boundary. (There are four such frequencies for fcc and five for bcc lattices.) R_c and R_s will be adjusted so as to minimize the mean-square deviation at these symmetry points. Phonon dispersion throughout the Brillouin zone is then uniquely determined by the theory.

An important characteristic of pseudopotentials[3] is an (effective) repulsive part created by the kinetic energy associated with orthogonalization to the localized wave functions of the ion. Usually such a term is deliberately introduced as a repulsive square well.[4] In the model described above this effect enters indirectly as a consequence of fitting the theory to the zone-boundary symmetry points. R_s invariably is somewhat smaller than one would anticipate for the last-filled electron shell. A small R_s allows the repulsive potential from the shell electrons to continue its rapid increase (with decreasing r) to smaller values of r. This behavior creates the extra "kinetic" repulsion found in all pseudopotential models. An alternative approach might include such a repulsive term as a separate entity (in addition to the core and shell potentials). Such a model could have *a priori* appeal, but it would double the number of adjustable parameters.

III. DIELECTRIC FUNCTIONS

Equations (3) and (4) involve three dielectric functions. These were derived in WO, but we shall review them here and include a correction for the effective mass of the conduction band. It is well known that the thermal mass m_{th} (determined from the electronic specific heat) is larger than the band mass m_b:

$$m_{th}=m_b(1+\lambda) , \quad (15)$$

where λ is the electron-phonon coupling parameter that appears in the theory of superconductivity.[5] However, the enhancement given by Eq. (15) occurs only within $\sim k_B\Theta_D$ of the Fermi energy. Consequently the enhancement plays a negligible role in the dielectric response of the entire conduction electron sea. The band-structure mass m_b, however, must be incorporated.

The core-core dielectric function $\epsilon_{cc}(q)$ is just the ordinary conduction-electron dielectric function (appropriate for test charges):

$$\epsilon_{cc}(q)=1+\frac{Q(q)}{1-G_+(q)Q(q)} , \quad (16)$$

where, with $x\equiv k/k_F$,

$$Q(q)=\frac{m_be^2f(x)}{\pi\hbar^2k_Fx^2} , \quad (17)$$

Note that we have used the band mass m_b instead of the free-electron mass m:

$$f(x)\equiv\frac{1}{2}+\frac{1-x^2}{8x}\ln\left|\frac{(1+x)^2+\delta}{(1-x)^2+\delta}\right| . \quad (18)$$

This function is the familiar one from degenerate Fermi-gas theory, where $\delta=0$. The singular behavior near $x=1$ leads to Kohn anomalies in phonon spectra. Such anomalies are rarely observed, perhaps on account of anisotropy of the Fermi surface. The small parameter δ is (heuristically) inserted in Eq. (18) to moderate the singular behavior. δ was taken to be zero except for Ca and Pb, 10^{-3}, Sr, 10^{-2}, and Yb, 2×10^{-2}. $G_+(q)$ is the spin-symmetric exchange (and correlation) local-field function.[6] A frequently employed form, suggested by Hubbard,[7] and having the correct behavior at $q=0$ and ∞ is,

$$G_+(q)=\frac{1.1x^2}{1+1.7x^2} . \quad (19)$$

Table I lists the experimental values of m_{th},[8] various estimates for λ,[9] and the band masses used in our calculations.

Exchange interactions between shell electrons and the conduction-electron sea are much smaller than those between conduction electrons alone.[10] Accordingly we employ a smaller local-field correction, γ_sG_+, (with $0\le\gamma_s<1$) where it is relevant. $\epsilon_{cs}(q)$ and $\epsilon_{ss}(q)$ were derived in WO:

TABLE I. Thermal-mass, λ, and band-mass values employed in the computed phonon spectra. Data for m_{th} is from Ref. 8 and from Ref. 9 for λ.

Metal	m_{th}/m	λ	m_b/m
Na	1.26	0.20	1.05
K	1.25	0.136	1.10
Rb	1.26	0.14	1.10
Cu	1.38	0.155	1.19
Ag	1.00	0.15	0.87
Au	1.09	0.165	0.94
Ca	1.90	0.25	1.52
Sr	2.00	0.19	1.68
Ba	1.40	0.14	1.23
Yb	2.00		1
Al	1.48	0.44	1.03
Pb	1.97	1.55	0.77

$$\epsilon_{cs}(q)=\frac{1+(1-G_+)Q}{1-(1-\gamma_s)G_+Q}\ , \tag{20}$$

and

$$\epsilon_{ss}(q)=\frac{1+(1-G_+)Q}{(1-(1-2\gamma_s+\gamma_s^2G_+)G_+Q}\ . \tag{21}$$

Except for Pb, Sr, and Ba, we found γ_s could be taken equal to zero. The foregoing dielectric functions are appropriate for phonons since their frequencies are very small compared to the conduction-electron plasma frequency ω_p. We remarked already that $\epsilon\approx 1-\omega_p^2/\omega^2$ should be used for the collective shell-exciton modes of Eq. (2).

The sums over reciprocal space were extended to a limit $L=h^2+k^2+l^2$ such that calculated frequencies converged to about one part in 10^3. For K and Rb, L was 100; for Pb, L was 169; for Na, L was 225; and for Al, L was 256. L was 144 for the seven remaining elements.

In the following section we shall discuss the results obtained for each element. In Table II we list the pseudo-ion parameters found by fitting the zone-boundary symmetry points. Also listed are the values of γ_s and the energies $\hbar\omega_L$ of the collective shell-exciton.

IV. ALKALI METALS: Na, K, AND Rb

Phonon spectra of alkali metals are very easy to fit with pseudopotential models.[11] Li is an exception, and we shall consider this metal in a separate study. (The phonon spectrum of Cs has not yet been measured.) It is necessary, of course, to verify that the pseudo-ion model described in Sec. II provides a good description for the alkalis.

A "problem" that arises is that *two* parameters are almost superfluous. With a continuous range of R_c, say, one can find matching values for R_s which provide excellent fits to the phonon data. To eliminate this ambiguity, we have required that the model fit also the frequency of the collective shell exciton. Vacuum-ultraviolet absorption in the alkali metals reveals this excitation.[12] The peak energy of the first far-ultraviolet absorption band corresponds to the collective oscillation of all electrons in the last-filled shell relative to the ion core. (This phenomenon is analogous to the giant electric-dipole resonance in nuclei, for which all the protons oscillate 180° out of phase with the neutrons.) The shell collective mode can also be *virtually* excited at frequencies well below its absorption frequency ω_L. It has been shown[13] that the resulting (dynamic) shell potential stimulates dramatic interband transitions in the near ultraviolet, and these transitions have been observed in K, Rb, and Cs.[14] The calculated frequencies $\hbar\omega_L$, shown in the last column of Table II, agree with the observed ones for Na, K, and Rb. For the other metals only zone-boundary phonon data was used to fix R_c and R_s.

Phonon data for the elemental metals are readily available.[15] Figure 1 shows the data[16] for K (from neutron scattering at 9°K). The slow shear mode along $[\xi\xi 0]$ has also been measured.[17] At the zone boundary its frequency is 0.55 THz. The dynamic pseudopotential fit is also shown. Only one free parameter is involved in the fit since, as described above; the other was used to fit the collective shell-exciton frequency. Phonon data and pseudo-

TABLE II. Pseudo-ion parameters R_c and R_s found by fitting the theory to measured phonon frequencies at zone-boundary symmetry points. Also listed is the shell-exchange parameter γ_s and calculated collective shell-exciton frequency.

Metal	Last-filled shell	$2k_FR_c$	$2k_FR_s$	γ_s	$\hbar\omega_L$ (eV)
Na	$2s+2p$	0.750	0.445	0	47.2
K	$3s+3p$	0.895	0.575	0	26.1
Rb	$4s+4p$	1.00	0.689	0	19.5
Cu	$3d$	1.62	0.993	0	37.5
Ag	$4d$	1.595	1.01	0	31.0
Au	$5d$	1.77	1.09	0	30.4
Ca	$3s+3p$	1.348	0.840	0	29.0
Sr	$4s+4p$	1.54	0.99	0.03	21.8
Ba	$5s+5p$	1.533	0.835	0.29	22.1
Yb	$4f$	1.728	1.01	0	25.5
Al	$2s+2p$	1.245	0.580	0	72.2
Pb	$5d$	2.18	1.35	0.03	28.7

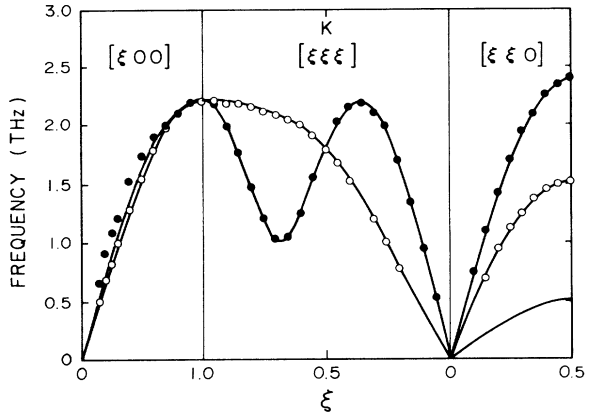

FIG. 1. Phonon spectrum of K at 9 K, due to Cowley *et al.*, Ref. 16. The curves are from a one-parameter fit.

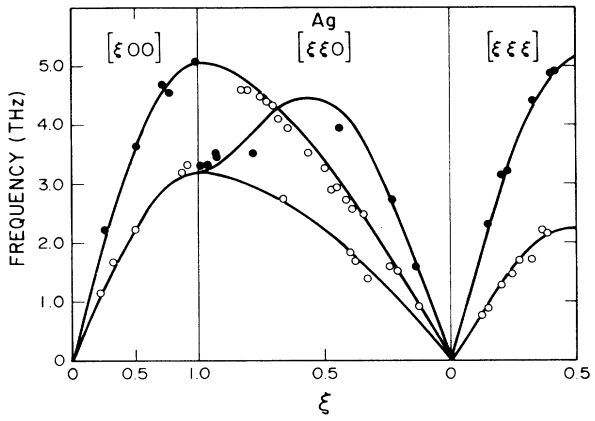

FIG. 3. Phonon spectrum of Ag at room temperature, due to Drexel, Ref. 18. The curves are a two-parameter fit.

potential fits for Na and Rb are so similar that we do not bother to show them. (The pseudo-ion parameters R_c and R_s are listed in Table II.)

It should be noticed that the last-filled shell for K was taken to be the $3s$ *and* $3p$, so $z=8$. The shell charge density, from Eqs. (7) and (9), is accordingly

$$\rho_s(r)\sim[1+(r/R_s)^2]\exp(-r^2/2R_s^2)\ . \tag{22}$$

A similar combination was used for six other metals, as indicated in Table II.

V. NOBLE METALS: Cu, Ag, AND AU

Phonon data[18] for Cu, Ag, and Au and the two-parameter theoretical fits are shown in Figs. 2–4. We believe the agreement is noteworthy for such a simple model. (There appears to be no need to introduce Born-Mayer repulsive forces, three-body forces, etc.) During the course of this research we have noticed that many two-parameter pseudopotential models fail to describe the spectra of noble metals. The key difference in the theory employed here is the recognition that the last-filled shell consists of d electrons. This feature leads to the r^4 factor in Eq. (11), without which we were unable to find a satisfactory solution.

An interesting feature of the data for Au is the *positive* dispersion of the slow-shear mode along [$\xi\xi$0]. The upward curvature in $\omega(q)$ also occurs in the theoretical fit (which involved data only at four zone-boundary points). We remark again, in reference to this phenomenon, that the dielectric function employed was based on conduction electrons having an isotropic and parabolic $E(\mathbf{k})$.

VI. DIVALENT METALS: Ca, Sr, Ba, AND Yb

The room-temperature phonon spectrum[19] of Ca and the theoretical fit are shown in Fig. 5. There appears to be no special feature needing comment.

Sr is fcc at room temperature but is bcc above 830 K. The solid-solid phase transition causes difficulty in growing large single crystals of the room-temperature phase. The phonon spectrum of the high-temperature phase was

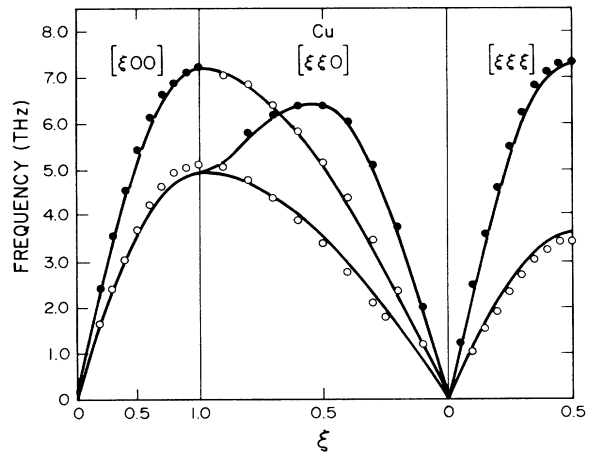

FIG. 2. Phonon spectrum of Cu at 49 K, due to Nicklow *et al.*, Ref. 18. The curves are a two-parameter fit.

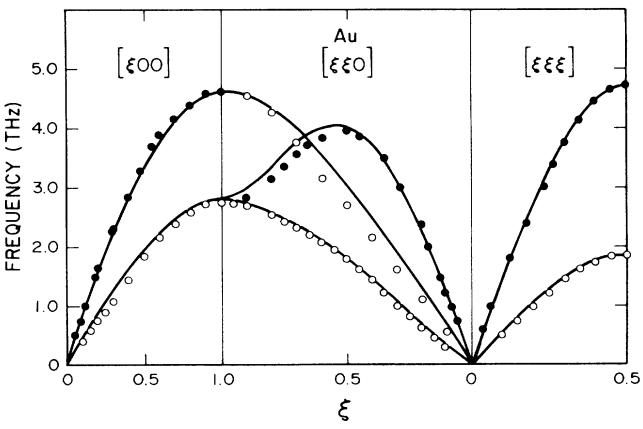

FIG. 4. Phonon spectrum of Au at room temperature, due to Lynn, *et al.*, Ref. 18. The curves are a two-parameter fit.

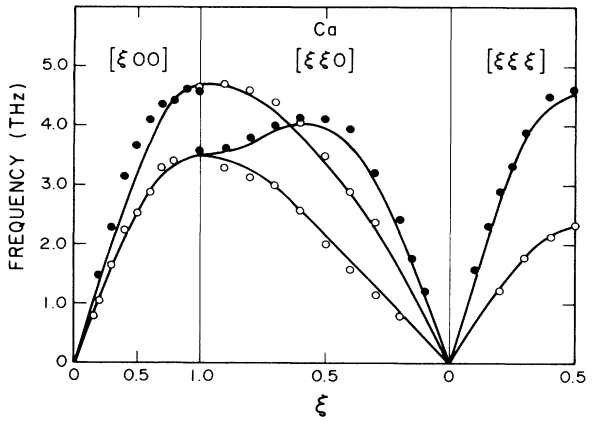

FIG. 5. Phonon spectrum of Ca at room temperature, due to Stassis, *et al.*, Ref. 19. The curves are a two-parameter fit.

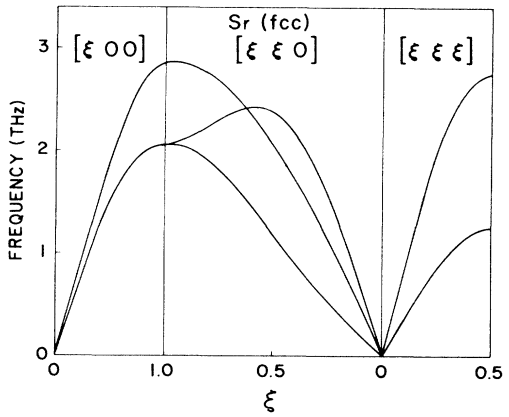

FIG. 7. Predicted spectrum of fcc Sr for the same atomic density as Fig. 6.

recently measured[20] at 930 K. The data and our theoretical fit are shown in Fig. 6. This is a three-parameter fit, since a small exchange coupling ($\gamma_s=0.03$) between the $4s$-$4p$ shell and the conduction-electron sea was incorporated. The same pseudo-ion parameters were used to predict the spectrum for the fcc phase, and the results are shown in Fig. 7. (No corrections for thermal contraction were made.) The spectrum has not been measured. Positive dispersion of the slow shear mode along [$\xi\xi$0] is predicted.

The room-temperature spectrum of Ba was determined recently[21] and is presented in Fig. 8. The solid curves of the figure were calculated from the theory with a shell-exchange parameter $\gamma_s=0.29$. Perhaps the most noteworthy feature of the spectrum is along the [ξ00] direction. The transverse mode lies higher than the longitudinal mode from $\xi=0$ to the zone boundary. The two dashed curves (for this direction) were calculated after setting $\gamma_s=0.20$. The longitudinal mode is then higher than the transverse. This result suggests that the longitudinal-transverse reversal can be attributed to strong exchange coupling between the Ba $5s$-$5p$ shell and the conduction-electron sea. This anomalous behavior has previously been attributed to hybridization of the conduction band with the (unoccupied) $5d$ band.[22] Alternatively, partial occupation of the $5d$ band has been suggested as the cause.[23] An interesting challenge is to find an experimental path to distinguish between these three theoretical explanations.

Lattice dynamics of the room-temperature phase[24] (fcc) of Yb is displayed in Fig. 9. The solid curves are a two-parameter theoretical fit. This metal is of interest because the last-filled shell is the $4f$ shell. It is interesting to observe that the positive dispersion of the slow-shear mode along [$\xi\xi$0] is given by the dynamic-pseudopotential model.

YB has a bcc phase above 935 K. Its phonon spectrum has not yet been measured. Figure 10 shows the predicted spectrum based on the same values of R_c and R_s found for the fcc phase. (No corrections for thermal expansion were included.) There are two noteworthy features of the spectrum shown in Fig. 10. The first is a crossing of the

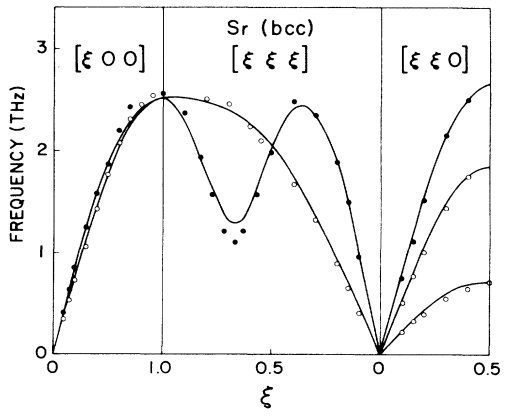

FIG. 6. Phonon spectrum of bcc Sr at 930 K, due to Mizuki and Stassis, Ref. 20. The curves are a three-parameter fit.

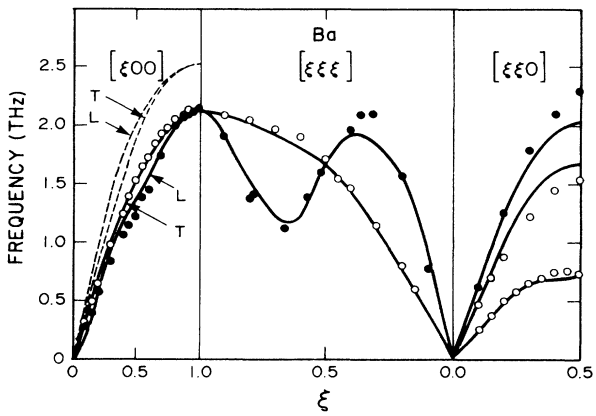

FIG. 8. Phonon spectrum of Ba at room temperature, due to Mizuki *et al.*, Ref. 21. The curves are a three-parameter fit.

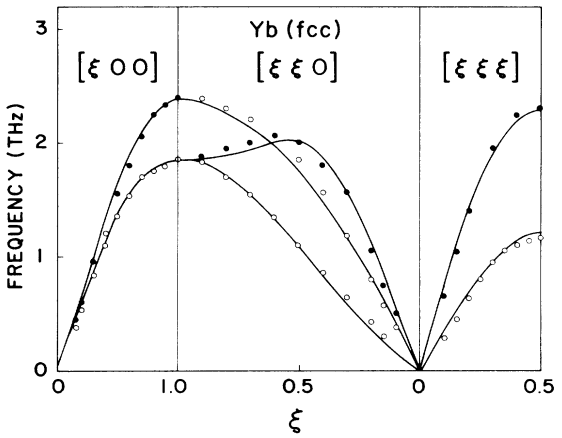

FIG. 9. Phonon spectrum of fcc Yb at room temperature, due to Stassis *et al.*, Ref. 24. The curves are a two-parameter fit.

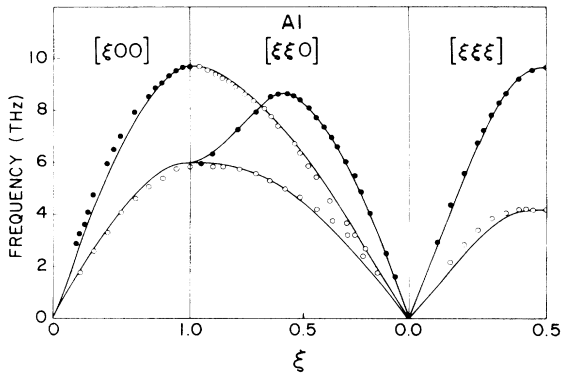

FIG. 11. Phonon spectrum of Al at 80 K, due to Stedman and Nilsson, Ref. 25. The curves are a two-parameter fit.

L and T modes along [ξ00]. The second is a peak in the slow-shear mode along [$\xi\xi$0]. Such an experiment seems feasible; it would provide an interesting test of the theoretical model.

VII. Al AND Pb

We conclude our study of cubic metals with trivalent Al and tetravalent Pb. The phonon spectrum[25] at 80 K in Al is shown in Fig. 11. The solid curves are a two-parameter fit. The agreement seems satisfactory.

Understanding the lattice-dynamics spectrum of Pb is a long-standing challenge. Data[26] at 100 K is shown in Fig. 12 along with a three-parameter fit. The dip in both L and T modes at the (100) zone-boundary point is not explained. This discrepancy is rather large, and a proportionate, possible cause has never been found. Reduction in the size of this anomaly at 290 K has been reported,[27] but independent work[28] at 300 K is conflicting.

At very speculative possibility is that the phonon spectrum near (100) is distorted by the occurrence of a charge-density-wave (CDW) broken symmetry[29] having a wave vector $\mathbf{Q}\approx(2,1,1)$. Elastic CDW diffraction satellites would then also appear near (100), but could be misinterpreted as order contamination, e.g., a $\lambda/2$ reflection from (200). Merging of the CDW phason spectrum[30] with the phonons would lead to anomalous $\omega(\mathbf{q})$ measurements near the CDW satellite locations. Such phenomena have been observed in K.[31] Investigation of this suggestion is an easy experimental task.

VIII. CONCLUSIONS

Application of the dynamic pseudopotential model to cubic metals (having one atom per primitive cell) indicates that a two parameter description of the phonon spectrum can usually be obtained. For Sr, Ba, and Pb inclusion of exchange coupling between the last-filled shell and the conduction-electron sea allows improved results. We do not know why such coupling, which is surely present in all metals, should not have been helpful generally. A pos-

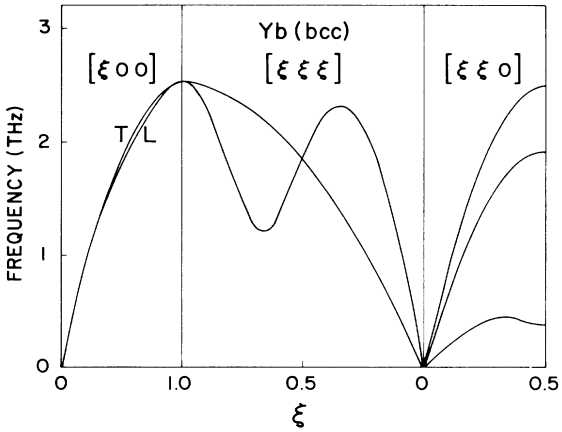

FIG. 10. Predicted spectrum of bcc Yb for the same atomic density as Fig. 9.

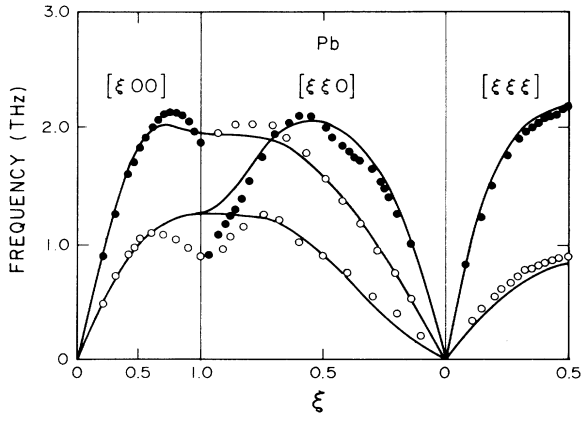

FIG. 12. Phonon spectrum of Pb at 100 K, due to Brockhouse *et al.*, Ref. 24. The curves are a three-parameter fit.

sible answer is that the shell potential, as discussed in Sec. II, includes (by default) the repulsive part of the pseudopotential associated with orthogonalization of conduction-electron wave functions to localized ion wave functions. Such (kinetic) "repulsion" would not involve exchange coupling.

An important feature of the dynamic-shell model is its allowance for ion deformation during vibration. To illustrate the magnitude of this effect we have computed zone-boundary phonon frequencies for each metal, keeping all parameters fixed, but requiring the core and shell amplitudes, A and B of Eq. (1), to be equal. The modes which suffered the largest increase in frequency are listed in Table III. It is clear that ion deformation is most important in the heavy metals.

The model can also be applied to metals with two or more atoms per primitive cell. For the hcp structure the dynamical matrix will be 12×12. There will be, of course, three acoustic-phonon solutions, three optic phonons, and six collective shell excitons (for each $\mathbf{q}$). Such a study has not yet been attempted.

Finally we want to emphasize the practical importance of the r^{2l} factors in the shell charge densities, Eqs. (9), (11), and (13), of the pseudo-ion model. Recognition of this fundamental aspect of angular-momentum wave functions was a key factor in the success of this investigation.

TABLE III. Maximum increase in the zone-boundary frequency when the ions are rigid.

Metal	Mode	Frequency increase
Na	$[0.5\,0.5\,0]\,T_{\text{fast}}$	0.2%
K	$[0.5\,0.5\,0]\,T_{\text{fast}}$	0.8
Rb	$[0.5\,0.5\,0]\,T_{\text{fast}}$	1.0
Cu	$[100]\,T$	7.5
Ag	$[100]\,T$	6.2
Au	$[100]\,T$	16.0
Ca	$[0.5\,0.5\,0.5]\,L$	3.5
Sr	$[0.5\,0.5\,0]\,L$	3.2
Ba	$[0.5\,0.5\,0]\,L$	3.5
Yb	$[0.5\,0.5\,0.5]\,T$	1.4
Al	$[100]\,L$	0.0
Pb	$[100]\,L$	57.0

ACKNOWLEDGMENT

We are grateful to the Division of Materials Research of the National Science Foundation for support for this program.

[1]Y. R. Wang and A. W. Overhauser, preceding paper, Phys. Rev. B **34**, 497 (1986).
[2]B. G. Dick and A. W. Overhauser, Phys. Rev. **112**, 90 (1958).
[3]W. A. Harrison, *Pseudopotentials in the Theory of Metals* (Benjamin, New York, 1966).
[4]V. Heine and I. Abarenkov, Philos. Mag. **9**, 451 (1965).
[5]G. Grimvall, *The Electron-Phonon Interactions in Metals* (North-Holland, Amsterdam, 1981).
[6]Carl A. Kukkonen and A. W. Overhauser, Phys. Rev. B **20**, 550 (1979).
[7]J. Hubbard, Proc. R. Soc. London, Ser. A **243**, 336 (1967).
[8]C. Kittel, *Introduction to Solid State Physics, Sixth Edition* (Wiley, New York, 1986), p. 141. The value of Au is from D. L. Martin, Phys. Rev. **170**, 650 (1968); the value for Yb is from D. V. Lounasmaa, Phys. Rev. **29**, 2460 (1963).
[9]A. H. MacDonald and C. R. Leavens, Phys. Rev. B **26**, 4293 (1982); G. Grimvall, Phys. Scr. **12**, 337 (1975); P. B. Allen and M. L. Cohen, Phys. Rev. **187**, 527 (1969); G. Grimvall, Physik Kondens. Mater. **11**, 278 (1970); R. C. Dynes and J. M. Rowell, Phys. Rev. B **11**, 1884 (1975).
[10]Y. R. Wang and A. W. Overhauser, Phys. Rev. B **34**, 6839 (1986).
[11]N. Ashcroft, J. Phys. C **1**, 232 (1968).
[12]S. Sato, T. Miyahara, T. Hanyu, S. Yamaguchi, and T. Ishii, J. Phys. Soc. Jpn. **47**, 836 (1979); H. Peterson and C. Kunz, Phys. Rev. Lett. **35**, 863 (1975).
[13]A. C. Tselis and A. W. Overhauser, Phys. Rev. Lett. **54**, 1299 (1985).
[14]U. S. Whang, E. T. Arakawa, and T. A. Collcott, Phys. Rev. B **6**, 2109 (1972).
[15]H. R. Schober and P. H. Dederichs, *Phonon Dispersion, Frequency Spectra, and Related Properties of Metallic Elements*, Vol. 13a of *Landolt-Börnstein* (Springer-Verlag, Berlin, 1981).
[16]R. A. Cowley, A. D. B. Woods, and G. Dolling, Phys. Rev. **150**, 487 (1966).
[17]J. Meyer, G. Dolling, J. Kalus, C. Vettier, and J. Paureau, J. Phys. F **6**, 1899 (1976); G. Dolling and J. Meyer, *ibid.* **7**, 775 (1977).
[18]R. M. Nicklow, G. Gilat, H. G. Smith, L. J. Raubenheimer, and M. K. Wilkinson, Phys. Rev. **164**, 922 (1967); W. Drexel, Z. Phys. **255**, 281 (1972); J. W. Lyon, H. G. Smith, and R. M. Nicklow, Phys. Rev. B **8**, 3493 (1973).
[19]C. Stassis, J. Zaretsky, D. M. Misemer, H. L. Skriver, B. N. Harmon, and R. M. Nicklow, Phys. Rev. B **27**, 3303 (1983).
[20]J. Mizuki and C. Stassis, Phys. Rev. B **32**, 8372 (1985).
[21]J. Mizuki, Y. Chen, K. M. Ho, and C. Stassis, Phys. Rev. B **32**, 666 (1985).
[22]Y. Chen, K. M. Ho, B. N. Harmon, and C. Stassis, Phys. Rev. B **33**, 3684 (1986).
[23]John A. Moriarty (unpublished).
[24]C. Stassis, C. K. Loong, and C. Theisen, Phys. Rev. B **26**, 4106 (1982).
[25]R. Stedman and G. Nilsson, Phys. Rev. **145**, 492 (1966).
[26]B. N. Brockhouse, T. Arase, G. Cagliotti, K. R. Rao, and A. D. B. Woods, Phys. Rev. **128**, 1099 (1962).
[27]A. Furrer and W. Hälg, Phys. Status Solidi **42**, 821 (1970).
[28]R. Stedman, L. Almquist, G. Nilsson, and G. Raunio, Phys. Rev. **162**, 545 (1967).
[29]A. W. Overhauser, Phys. Rev. **167**, 691 (1968).
[30]A. W. Overhauser, Phys. Rev. B **3**, 3172 (1971).
[31]T. M. Giebultowicz, A. W. Overhauser, and S. A. Werner, Phys. Rev. Lett. **56**, 1485 (1986).